The nightside-to-dayside evolution of the inner magnetosphere: Imager for Magnetopause-to-Aurora Global Exploration Radio Plasma Imager observations

H. S. Fu,[1,2,3] J. Tu,[1] P. Song,[1] J. B. Cao,[2] B. W. Reinisch,[1] and B. Yang[1,4]

Received 20 July 2009; revised 17 October 2009; accepted 19 November 2009; published 23 April 2010.

[1] It took about 12 h for the Imager for Magnetopause-to-Aurora Global Exploration (IMAGE) satellite to fly from the outbound pass to inbound pass of every inner magnetosphere crossing. This provides a unique opportunity to study the nightside-to-dayside evolution of the corotating inner magnetosphere when the outbound pass is in the nighttime while the inbound pass is in the daytime because a flux tube observed on the nightside may be observed again on the dayside in such situation. The differences between the two observations may be caused by the evolution of the flux tube. By analyzing both the passive and active sounding measurements from the IMAGE Radio Plasma Imager, we study two cases concerning this evolution. One, under a quiet geomagnetic condition, shows a typical evolution process during which the plasmapause was observed on both the nightside and the dayside. The other, during the recovery phase of a magnetic storm, shows a different inner magnetospheric structure in which the distinct plasmapause observed on the nightside becomes unidentifiable on the dayside as the density in the nearly empty nightside plasmatrough increases to a level similar to that of the plasmasphere. It is shown that the evolutions of the inner magnetosphere in both cases were primarily controlled by the fast plasma refilling of the flux tubes from the ionosphere as the flux tubes drift from the nightside to the dayside. In the former case the fast refilling was confined inside L = ~6.3, while in the latter case the fast refilling extended to at least L = 10. The present observations provide an example for fast refilling as a possible cause of the smooth density transition from the plasmasphere to the subauroral region and demonstrate the importance of the plasmasphere-ionosphere coupling in controlling the structures of the inner magnetosphere.

Citation: Fu, H. S., J. Tu, P. Song, J. B. Cao, B. W. Reinisch, and B. Yang (2010), The nightside-to-dayside evolution of the inner magnetosphere: Imager for Magnetopause-to-Aurora Global Exploration Radio Plasma Imager observations, *J. Geophys. Res.*, *115*, A04213, doi:10.1029/2009JA014668.

1. Introduction

[2] The plasmasphere, a major structure of the inner magnetosphere, is a vast toroidal region of cold (temperature ≤1 eV) and dense (10^2–10^4 cm^{-3}) plasma of ionospheric origin. It encircles Earth and extends from the topside ionosphere (about 1000 km in altitude) out to equatorial altitudes ranging from about 10,000 to 40,000 km, where it reaches its outer boundary, known as the plasmapause [*Lemaire and Gringauz*, 1998]. The plasmapause is a transition layer with an abrupt drop of the equatorial plasma density from 100 to 1000 particles cm^{-3} down to a few particles per cubic centimeter [*Carpenter*, 1963], and it is believed to be caused by the interplay of Earth's corotation and magnetospheric convection [*Nishida*, 1966]. Usually an equatorial density decrease of more than a factor of 5 over a region of less than 0.5 L is regarded as the signature of the plasmapause [*Carpenter and Anderson*, 1992]. Outside the plasmapause is the plasmatrough, a region filled with hot (~100 eV to 100 keV) and tenuous (~1 cm^{-3}) plasma [e.g., *Frank*, 1971; *Thomsen et al.*, 1998; *Carpenter and Lemaire*, 2004]. Inside the plasmapause the flux tubes drift on closed paths around Earth, allowing long-time refilling of the cold plasma from the underlying ionosphere to build up high density in the plasmasphere [e.g., *Singh and Horwitz*, 1992]. Beyond the plasmapause, however, the flux tubes convect sunward (therefore are on open drift paths) and drain their content of plasma along the open field lines to the interplanetary space as a result of reconnection of the magnetospheric and interplanetary magnetic fields at the magnetopause, resulting in lower plasma densities in the trough region [e.g., *Carpenter and Lemaire*, 1997].

[1]Center for Atmospheric Research, University of Massachusetts Lowell, Lowell, Massachusetts, USA.
[2]State Key Laboratory for Space Weather, Center for Space Science and Applied Research, Beijing, China.
[3]Graduate University, Chinese Academy of Sciences, Beijing, China.
[4]Also at Institute of Space Physics and Applied Technology, Peking University, Beijing, China.

0148-0227/10/2009JA014668

[3] The flux tubes drifting on both the closed and open paths may experience plasma refilling when the flux tubes drift from the nightside to the dayside. It usually takes several to tens of days, depending on the L shell, for the plasmaspheric density to reach the saturated or "filled" density level after the density depletion during magnetic storms [e.g., *Singh and Horwitz*, 1992, and references therein]. For instance, *Park* [1970] found that the "empty" tubes at $3.5 < L < 5$ eroded in a storm took about 5 days to reach the monthly median values, and even after 8 days of quiet conditions the refilling continued. *Reinisch et al.* [2004] observed the fast refilling of the flux tubes in the L shell range of 2.0–3.5 by analyzing the sounding measurements made by the Imager for Magnetopause-to-Aurora Global Exploration (IMAGE) Radio Plasma Imager (RPI) during a great magnetic storm. The refilling time for the flux tubes to refill from 30% full to full is still greater than 1 day, about 28 h. Let us look more carefully at the importance of the speed of refilling. The flux tubes on the newly closed drifting paths can continuously accumulate plasma to reach a saturated density level, while the time for the flux tubes on the open drifting paths to refill is limited by the nightside-to-dayside drift time. If the refilling is slow, the flux tubes on the open drift paths will not accumulate significant plasma, so that the plasmatrough density on the dayside is expected to be as low as that in the nightside trough. In this case, the plasmapause is expected to exist on both the nightside and dayside, although its location may change due to the varying magnetospheric convection. If, on the other hand, the refilling time scale is comparable to or faster than the time scale for the flux tube to drift from the nightside to the dayside, an empty flux tube on the nightside would be refilled after it drifts to the dayside. In this case, the plasmapause can be observed on the nightside but perhaps not on the dayside.

[4] Under normal conditions, the refilling may be slow, and the structure of the inner magnetosphere is basically the same during the 1 day (or less) evolution. Such a structure was predicted by the seminal work of *Nishida* [1966] and has been demonstrated by numerous observations and modeling studies [e.g., *Singh and Horwitz*, 1992; *Lemaire and Gringauz*, 1998; and references therein]. The recent modeling study by *Pierrard and Stegen* [2008], which includes an additional process, namely the interchange instability, to the interplay of the corotation and convection as a mechanism of the plasmapause formation, also showed that the plasmapause persists when the plasmasphere corotates with Earth.

[5] Nevertheless, the near-equatorial ISEE 1 observations by *Nagai et al.* [1985] have shown that the classical plasmapause determined by the sharp density gradient was not always observed in the dayside region; that is, the density profiles were smooth on occasion. *Carpenter and Anderson* [1992] used the electron density profiles also obtained by the ISEE 1 satellite to demonstrate that after 4 days of the refilling the plasmasphere with a well-defined plasmapause became an extended dense plasmasphere at the magnetic local time (MLT) sector sampled by the ISEE 1. On the basis of the observations of the RPI on board the IMAGE satellite, *Tu et al.* [2007] recently showed that during the geomagnetic quiet periods the smooth density profiles can extend from the inner plasmasphere to the subauroral region and can occur at various local times. The causes of the smooth transitions, or the absence of the plasmapause, however, have not been clearly revealed.

[6] One possible cause is that during a prolonged period of extreme quiet geomagnetic condition the corotation is dominant over an extended spatial range. It is also possible that the plasmaspheric wind advocated by *Lemaire and Schunk* [1992] takes effect during a prolonged quiet period. The plasmasphere is expected to extend on both the nightside and dayside due to any one of above two processes. The smooth transitions observed by *Tu et al.* [2007] might result from those processes because on both the nightside and the dayside electron density distributions were observed to smoothly transit from the plasmasphere to the subauroral region. Another situation in which the plasmapause can be clearly seen on the nightside but the density distributions become smooth on the dayside is that the plasmaspheric structure changes in a time scale of about 0.5 day, roughly the time period for the plasmasphere to corotate with Earth from the nightside to the dayside.

[7] In this study we investigate such short-time evolution of the inner magnetospheric structure using the measurements by RPI on the IMAGE satellite together with observations by the Defense Meteorological Satellite Program (DMSP) satellites. Two cases are examined in detail. One, under quiet geomagnetic conditions, displays typical characteristics of the evolution that the plasmapause exists on both the nightside and dayside. The other case, observed during the recovery phase of a magnetic storm, shows different features. In this case, when the nearly "empty" flux tubes in the nightside plasmatrough drifted to the daytime region, the plasma density in the flux tubes was increased to the level making the preexisting distinct plasmapause disappear. In section 2 we briefly describe the observation data from IMAGE RPI and DMSP. In section 3 the two observational cases are analyzed in detail, and section 4 gives the discussions and summary.

2. Data and Methods

[8] The IMAGE satellite [*Burch et al.*, 2001] was in a polar orbit with a period of 14.2 h so that it traversed the plasmasphere and plasmatrough region about twice a day. The RPI [*Reinisch et al.*, 2000] on board IMAGE operated alternately between making passive radio wave measurements and active sounding measurements. In the active sounding mode RPI transmitted coded signals and listened to the echoes, stepping through the frequencies within the range of 3 kHz to 3 MHz. The signal intensities of these received echoes are displayed as a function of frequency and echo delay time (represented as virtual range: one half of the echo delay time multiplied by the speed of light in free space) in a plasmagram, as shown in Figure 1. In the plasmagram, usually the electron cyclotron (f_{ce}), the upper hybrid (f_{uh}), and the plasma frequency (f_{pe}) can be clearly identified. Multifrequency echoes form a distinct X-mode trace, whose cutoff frequency at the satellite location, that is, f_x, can also be well identified. It has been shown that the X-mode trace obtained in the magnetosphere represents the reflected signals propagating along the magnetic field line intersecting the satellite [*Reinisch et al.*, 2001; *Song et al.*, 2004; *Fung and Green*, 2005; *Fu et al.*, 2010]. Using the trace in a plasmagram, we can derive the field-aligned distribution of the

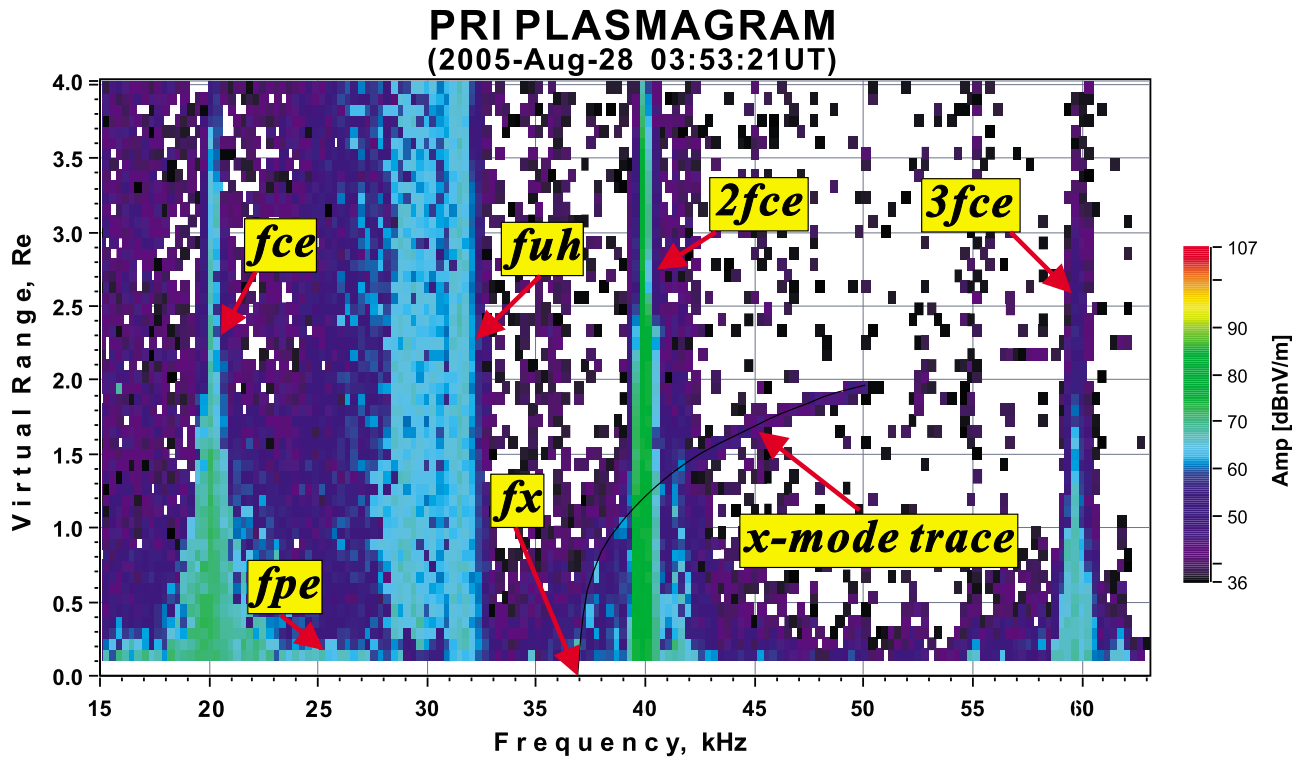

Figure 1. A plasmagram recorded by Imager for Magnetopause-to-Aurora Global Exploration (IMAGE) Radio Plasma Imager (RPI) at 0353:21 UT on 28 August 2005, displaying the amplitude (in dBnV m^{-1}) of received signals as function of frequency and time delay expressed in terms of virtual range. The local electron cyclotron (f_{ce}, $2f_{ce}$, $3f_{ce}$), upper hybrid (f_{uh}), and plasma (f_{pe}) frequencies are identified as the vertical intense signals. The *X*-mode trace and its cutoff frequency (f_x) are detected as well.

electron density by applying an inversion algorithm [*Huang et al.*, 2004]. The trace in Figure 1 will be analyzed in detail in section 3.2. In the passive measurement mode RPI monitored the natural plasma wave environment around the satellite. Those natural plasma wave signals are displayed in conventional frequency-time electric field spectrograms (referred to as dynamic spectra; see Figure 2) [*Green and Reinisch*, 2003] with the analysis software known as BinBrowser [*Galkin et al.*, 2004]. The upper hybrid resonance (UHR) band, a typical feature on the dynamic spectrograms, provides the information of the local electron density because the lower cutoff frequency of the UHR band is approximately the electron plasma frequency f_{pe} [e.g., *Mosier et al.*, 1973; *Shaw and Gurnett*, 1980].

[9] In this study, we first use the passive mode measurements to obtain the in situ electron density variations along the IMAGE orbits. Such electron density variations reflect the structure of the inner magnetosphere; that is, the electron density distribution either displays distinct signatures of the plasmapause or varies smoothly from the inner plasmasphere to the subauroral region. The measurements made by RPI in the years 2001 and 2005 are examined to select events for the study of the inner magnetosphere from the nightside to dayside. In these years the inbound pass and outbound pass orbit segments are roughly symmetric about the geomagnetic axis, providing a contrast of the plasmaspheric density profiles at similar magnetic latitudes but at opposite MLT sectors. In addition, the time difference between the inbound and outbound passes is about 12 h in these 2 years, comparable with the corotation period of the plasmasphere. Therefore, IMAGE intersected roughly the same flux tubes on its inbound and outbound passes. In our cases, they were on the nightside and dayside, respectively. The available active sounding measurements are also used to derive the field-aligned density distributions so that the equatorial density can be inferred. From the equatorial density the plasmasphere refilling rate may be estimated.

[10] In order to determine the source of refilling, we use DMSP satellite data to monitor the upward fluxes from the ionosphere. The DMSP is a constellation of satellites circling Earth in Sun-synchronous orbits at ~850 km altitude with orbit periods of ~104 min. We analyze the data from the retarding potential analyzer (RPA) and the ion drift meter (IDM) on board the DMSP satellites. The RPA provides the ion density, ion temperature, ram ion velocity, and ion composition in the topside ionosphere, while the IDM measures the vertical and horizontal (cross track) components of the plasma velocity in the range of ±3000 m s^{-1} (corresponding to a maximum energy of 0.75 eV for an O^+ ion). In the present study, the ion density, ion composition, and vertical velocity with a temporal resolution of 4 s are presented to coordinate with the IMAGE RPI observations. The DMSP satellites and the measurement techniques have been described in detail by *Hairston and Heelis* [1990].

[11] To correlate and compare the measurements from the nightside and dayside, we trace the motion of the flux tubes

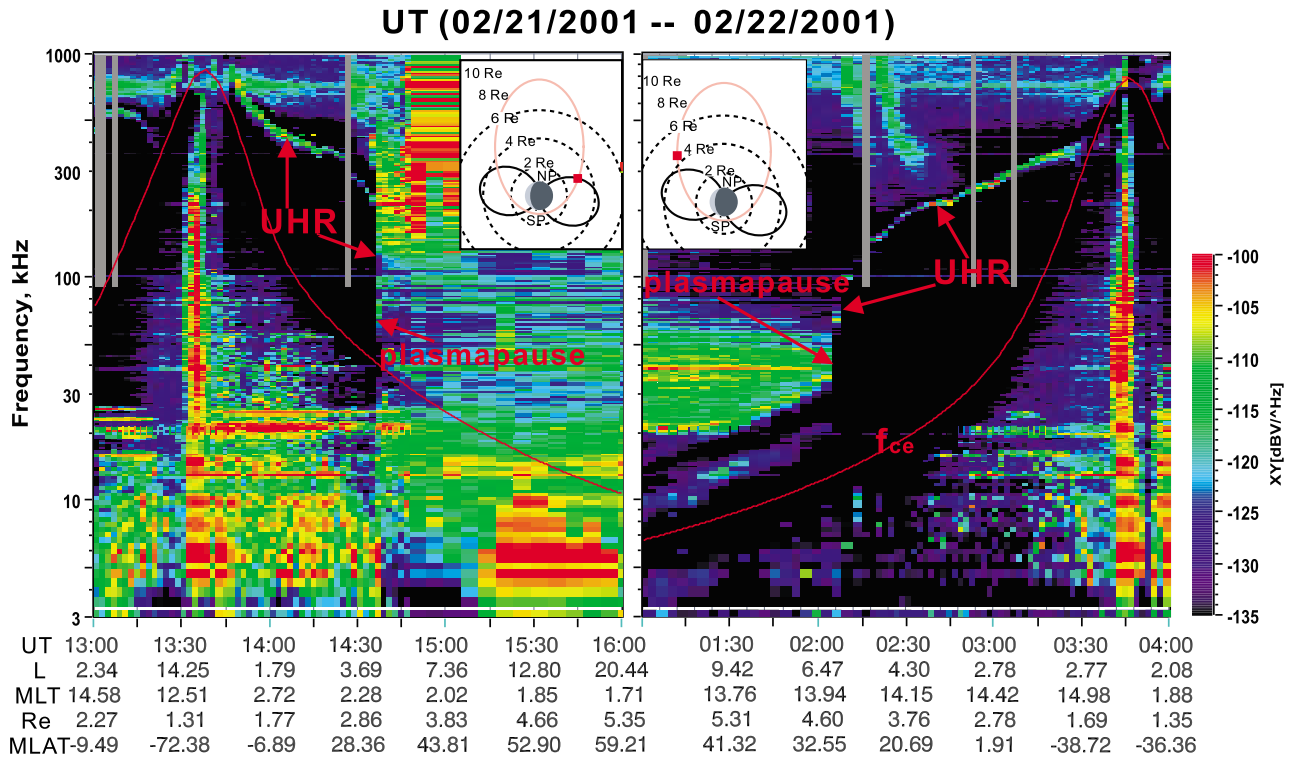

Figure 2. The dynamic spectra obtained by the IMAGE RPI during two consecutive traverses of the plasmasphere-plasmatrough. (left) The nightside outbound traverse from 1300 to 1600 UT on 21 February 2001. (right) The dayside inbound pass from 0100 to 0400UT on 22 February 2001. The time difference of the two passes is ~12 h. The red line represents the electron gyrofrequency determined by the T96 magnetic field model [*Tsyganenko*, 1995], and the vertical gray strips indicate data gaps. The satellite orbit configuration is shown in the insets, in which the shaded area of Earth indicates the nightside.

using the E5D model of electric field, which is determined by the simultaneous K_p index [*McIlwain*, 1986; *Pierrard and Stegen*, 2008], and the T96 model of the magnetospheric magnetic field [*Tsyganenko*, 1995]. The drift velocity of the flux tubes is calculated by $\boldsymbol{v} = \boldsymbol{E} \times \boldsymbol{B}/\boldsymbol{B}^2$, where the electric field $\boldsymbol{E}$ includes the contribution from the corotation with Earth and the magnetospheric convection.

3. Evolution of Plasmaspheric Structure

[12] In this section, we present two cases illustrating the evolution of the plasmaspheric density profiles from the nightside to the dayside. One case presents a typical situation, and the other case was observed in a storm recovery phase showing a completely different evolution of the plasmaspheric structure. Both cases were observed under quiet geomagnetic condition in terms of K_p values.

3.1. Case of 21–22 February 2001

3.1.1. Imager for Magnetopause-to-Aurora Global Exploration (IMAGE) Radio Plasma Imager (RPI) In Situ Measurements

[13] Figure 2 shows two sequential dynamic spectra measured by IMAGE RPI on 21–22 February 2001. The time difference between the outbound pass in nighttime (Figure 2, left) and the inbound pass in daytime (Figure 2, right) is about 12 h. The IMAGE orbit is schematically displayed in two insets in the dynamic spectra. The red squares in these insets represent the locations at which the satellite encountered the plasmapause, and the black lines denote the magnetic field line of $L = 4.3$. The satellite's orbits in the outbound pass and inbound pass of the inner magnetosphere are generally symmetric about the geomagnetic axis. The red curve in the spectra is the electron cyclotron frequency f_{ce} calculated with the T96 model [*Tsyganenko*, 1995]. The orbit information, including the L shell, MLT, radial distance in Earth radius (R_E), and the magnetic latitude (MLAT) are labeled below the abscissa of Figure 2. We can see clearly the UHR bands in these two dynamic spectra. The plasmapause, which appears as a steep gradient of the frequency of the UHR band, is marked in each spectrogram of Figure 2. From the lower-frequency cutoff of the UHR band, the electron densities can be derived [e.g., *Mosier et al.*, 1973; *Shaw and Gurnett*, 1980; *Benson et al.*, 2004].

[14] The variations of the derived electron density along the satellite orbits are presented in Figure 3. Figures 3a and 3b show, respectively, the derived electron densities on the nightside (outbound pass) and dayside (inbound pass) as functions of universal time. Figure 3c presents the density variation with the L shell, and Figure 3d shows the MLAT information along the orbits. Again, the density measurements shown in Figures 3a and 3b have a time separation of about 12 h. A sharp drop in the electron density changing from 599 to 25 cm^{-3}, nearly a factor of 24 over a distance less than 0.5 L, is clearly seen on the nightside at about 1436 UT (Figure 3a). Because the measurements were not made in the

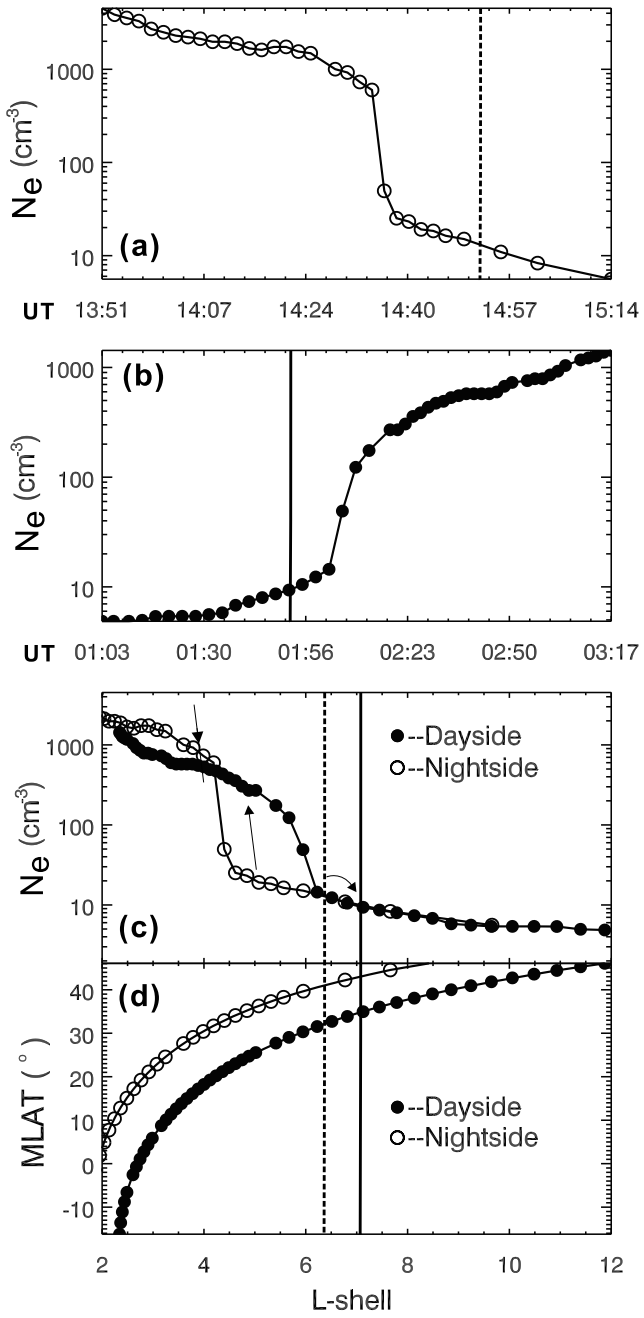

Figure 3. Density profiles derived from the dynamic spectrogram shown in Figure 2 as a function of (a, b) universal time and (c) L shell. (d) The magnetic latitude and L shell of the IMAGE locations. The open circles represent measurements on the nightside, and the solid circles represent measurements on the dayside. The vertical dash lines indicate the location of a flux tube on the nightside whose drift path is traced using the E5D electric field model [*McIlwain*, 1986] and the T96 magnetic field model [*Tsyganenko*, 1995]. The solid vertical lines represent the final location of that traced flux tube. The curved arrow in Figure 3c illustrates the change of the L shell of the traced flux tube. The straight arrows in Figure 3c denote two other traced flux tubes.

equatorial plane, the observed density change in time series data also includes the contribution from the latitudinal density variations. Nevertheless, we can see from the IMAGE orbits (insets in Figure 2) that the major contribution to the density change should be due to the density variations in L shell because the orbit is at large angles with respect to the field lines. Furthermore, and more important, it is difficult to attribute such sudden density change to the density variations along the field lines because the diffusion along the field lines does not support such a large density gradient along a field line. Thus the sharp density drop indicates the existence of the plasmapause. On the dayside a plasmapause with a density drop from 123 to 14 cm^{-3} over a distance less than 0.5 L was observed at ~0206 UT (Figure 3b). This density change is more than a factor of 8. The plasmapause is even more evident when the profiles are plotted as a function of L shell in Figure 3c, which compares the nightside (open circles) and dayside (solid circles) density distributions. We find from this comparison that the electron densities are almost the same in both the nightside and dayside plasmatrough. However, when considering that the IMAGE orbit was at slightly lower MLATs on the dayside (see Figure 3d), the same-MLAT electron density on the dayside region should be slightly larger. From nighttime to daytime, the plasmaspheric density decreased slightly in the plasmasphere. The plasmapause relocated outward from L = ~4.3 to ~5.8.

[15] The large increase in the distance of the plasmapause is very interesting. It can be attributed to either the outward motion of the plasmapause itself or the plasma refilling in the region that most recently became a part of the plasmasphere. According to *Carpenter and Anderson* [1992, Figure 10], the expansion from the nightside to dayside is typically 0.5 R_E, which may be too small to account for the 1.5 R_E difference in this case. Nevertheless, we still need to investigate this possibility.

3.1.2. Tracing the Motion of the Flux Tube

[16] In order to correlate the measurements from the nightside with those from the dayside, we consider the drift of a flux tube from the nightside to the dayside by using the E5D model, in which the electric field varies with time according to the K_p index and the T96 model, in which the magnetic field varies with the solar wind and interplanetary magnetic field (IMF) conditions. These solar wind conditions and also the geomagnetic indices are shown in Figure 4, where, from top to bottom, the K_p and D_{st} indices, IMF B_z, and ram pressure of the solar wind measured by ACE at X_{GSM} = ~230 R_E on 21–22 February 2001 are displayed, respectively.

[17] We first trace a flux tube just inside the nightside plasmapause encountered by IMAGE. The tracing begins at 1432 UT on 21 February 2001 and ends at 0237 UT the next day. The ending time is chosen as the time when the flux tube is closest to the IMAGE satellite orbit projection in the dayside equatorial plane. The tracing time step is set to be 1 min, and the tracing results in the solar magnetic (SM) coordinates are presented in Figures 5a and 5b. Figure 5a displays the initial location (as a triangle) of the flux tube in the equatorial plane of the SM coordinates at 1432 UT together with the electric equipotential lines (determined by the E5D model) at that time. Figure 5b shows the traced drift trajectory (thick solid line) imposed on the equipotential

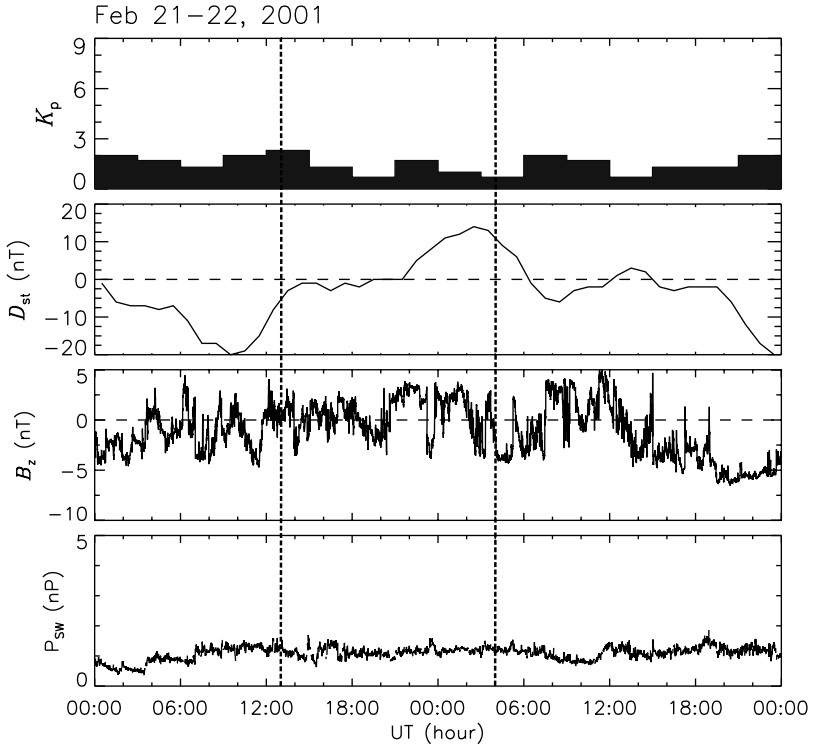

Figure 4. (top to bottom) K_p, D_{st} index, IMF B_z, and the solar wind dynamic pressure from 0000 UT on 21 February 2001 to 2400 UT on 22 February 2001. The two vertical dashed lines denote the interval of the IMAGE RPI observations shown in Figure 2.

lines at 0237 UT. The differences of the equipotential lines between Figures 5a and 5b are due to the differences in K_p index and the solar wind conditions. The dash-dotted line in Figure 5 denotes the satellite orbit mapped to the equatorial plane along the magnetic field lines as specified by the T96 model. The equatorial plane projection of the IMAGE location at this time (0237 UT in Figure 5b) is labeled with a dot in Figure 5, while the flux tube location at this time is labeled with a rectangle. It is seen that the L shell of this traced flux tube does not change much from the nightside to dayside (represented with the left-pointing downward arrow in Figure 3c). Therefore, we may conclude that the expansion associated with corotation of the plasmasphere is unlikely to produce a radial outward shift of the plasmaspheric flux tubes when they drift around Earth from the nightside to the dayside. Note that the ending location of the flux tube (represented by a rectangle) is not exactly coincident with the IMAGE orbit projection at 0237 UT (represented by a dot in Figure 5), but the differences of local time and L shell between the two are small.

[18] Next we consider the flux tube that was initially just outside the nightside plasmapause. For this flux tube, tracing begins at 1442 UT on 21 February and ends at 0222 UT on 22 February. The starting time is when IMAGE encountered the flux tube, and the ending time is again chosen to make the closest distance between the IMAGE orbit plane and the flux tube ending location in the equatorial plane. The tracing results are displayed in Figures 5c and 5d in the same format as in Figures 5a and 5b. The flux tube is initially just outside the nightside plasmapause or in the region of the open drift paths (see Figure 5c). It then drifts to inside the dayside plasmasphere (the region of the closed drift paths) at 0222 UT on 22 February. This indicates that there is possibly reduction of the convection during the period of the flux tube drift from the nightside to the dayside. The reduction of the convection is consistent with the general declining trend of the K_p index as shown between the two vertical lines in Figure 4. It is seen that the L shell of this flux tube does not change significantly, from $L = 5.0$ to 4.9, while it drifts from the nightside to dayside, as represented by the middle upward arrow in Figure 3c. Again the differences, particularly the difference in the L shell, between the ending location of the flux tube, represented by a square in Figure 5d, and the IMAGE location at 0222 UT, indicated as a dot in Figure 5d, is small. It is thus reasonable to state that the flux tube actually encountered by the IMAGE at 0222 UT (on the dayside) experiences only a slight L shell change when it drifts from the nightside to the dayside, as does the flux tube traced. This indicates that the cause of the larger area of the outer plasmasphere on the dayside compared to that of the nightside plasmasphere may be the refilling process in flux tubes.

[19] One may argue that the plasmapause should be asymmetric between the nightside and dayside. It usually locates at larger L shell in the dayside than in the nightside due to the magnetospheric convection. This asymmetry actually has been considered in the E5D model of electric field. For instance, the plasmapause determined by the E5D model at 1432 UT on 21 February (Figure 5a) are at L = ~4.4 and ~5.0, respectively, in the postmidnight and postnoon sector, that is, about a difference of 0.6 R_E, consistent with the observations of *Carpenter and Anderson* [1992]. Although the E5D model we use is standard and

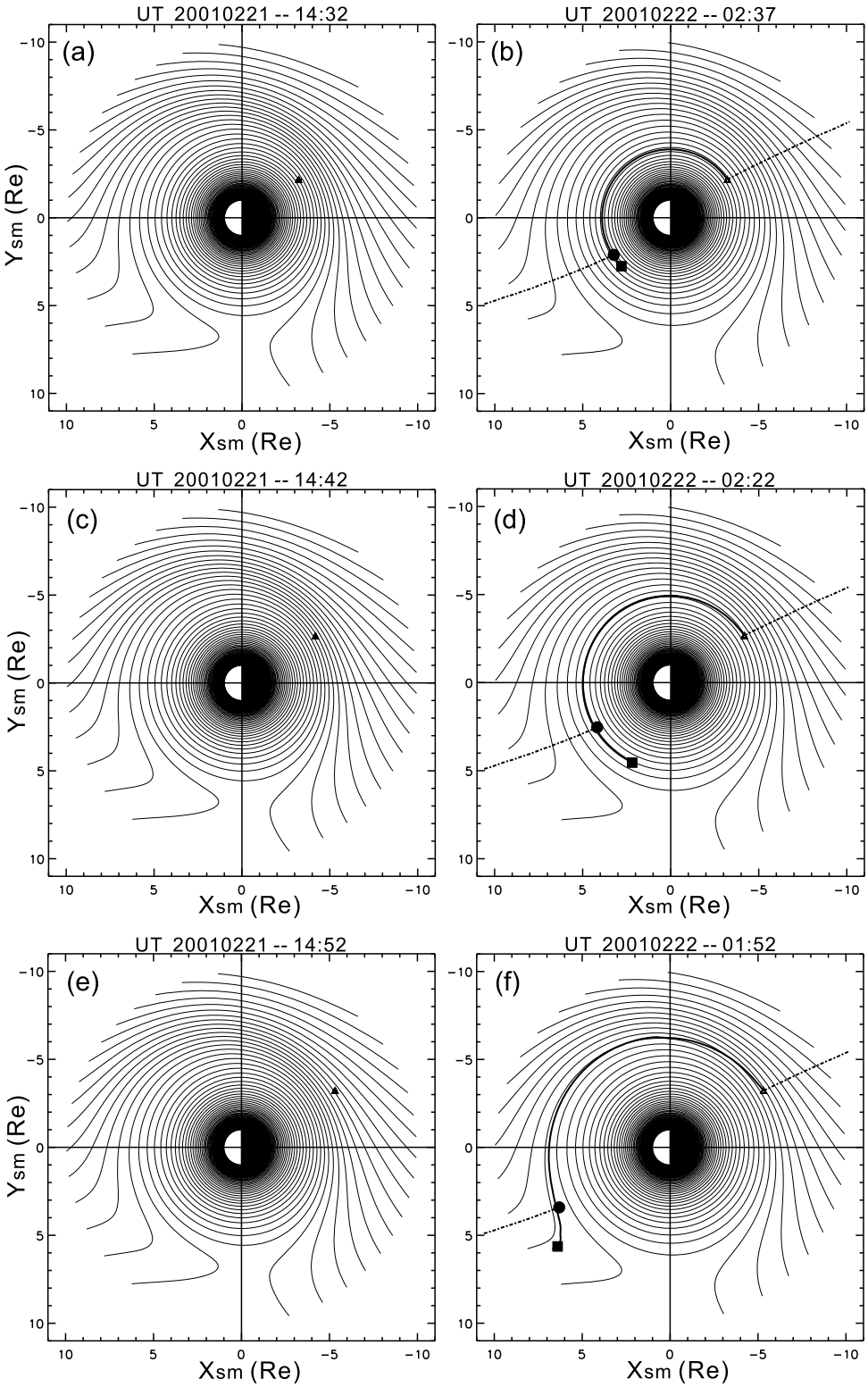

Figure 5. Drift trajectory tracing of three flux tubes initially located (a) just inside and (c) just outside the nightside plasmapause and (e) at the nightside geosynchronous orbit. Their L shell change from the nightside to the dayside is schematically represented by the left straight, middle straight, and right curved arrows in Figure 3c. (a, c, e) The initial location of each flux tube in the solar magnetic (SM) equatorial plane. (b, d, f) The trajectories (bold solid lines) imposed on the electric equipotential determined by the E5D model at the ending times of the trajectory tracing. The dot-dashed line is the equatorial projection, along the magnetic field lines, of the IMAGE orbit. The dot and rectangle represent, respectively, the locations of IMAGE projected to the SM equatorial plane and the traced flux tube at the tracing ending time.

has been widely used in the field, one may still argue that the method is not accurate and that the plasmapause drifts outward more than the model prediction. In this case the plasmapause could be farther out on the dayside than on the nightside, although the large outward relocation, 1.5 R_E, is beyond any reasonable model prediction. In order to validate our interpretation that the outward relocation of the plasmapause may be due to a fast refilling of the plasmatrough when the flux tubes rotated from the nightside to the dayside, we examine and present later in this section evidence for the source of refilling from the DMSP observations at the topside ionosphere.

3.1.3. Equatorial Densities

[20] In the present case, the plasmasphere became larger on the dayside with a clearly defined plasmapause. Beyond the dayside plasmapause there is only a slight change in the density from the nightside to dayside, as demonstrated by Figure 3c. Although one may think that there is no apparent density change in those flux tubes, as shown above, there is also a latitude effect due to the satellite orbit; see Figure 3d. If one compares the density at the same magnetic latitude, as to be shown later, one would observe a higher density on the dayside; that is, there is to some degree a refilling in the flux tubes beyond the dayside plasmapause.

[21] In order to determine the plasma refilling rate we need to estimate the equatorial densities of a given flux tube at nighttime and daytime as the densities shown before were measured at varying latitudes. We first infer the variations of the equatorial density with L values in the nightside and dayside local time sectors intersected by IMAGE, using the field-aligned density distributions derived from the IMAGE RPI sounding measurements [*Huang et al.*, 2004; *Reinisch et al.*, 2004; *Song et al.*, 2004; *Tu et al.*, 2006; *Fu et al.*, 2010]. We then use such variations to estimate the equatorial density of a given flux tube. It has been shown by *Tu et al.* [2006] that the field-aligned density profiles in the plasmasphere and plasmatrough can be represented by the following function form:

$$N_e = N_0(L)\cos^{-\beta(L)}\left(\frac{\pi}{2}\frac{\alpha(L)\lambda}{\lambda_{in}}\right),\ \alpha(L) = A + BL,\ \beta(L) = C + DL, \tag{1}$$

where λ and λ_{in} are the magnetic latitude along a field line and the invariant latitude of the field line, respectively. $N_0(L)$ is the minimum electron density of the RPI-measured density profiles, which is the in situ electron density at the satellite location. Parameter α (L) describes the steepness of the density profiles at high latitudes, while β (L) specifies the flatness of the profiles at low latitudes. The fitting parameters A, B, C, and D are to be determined by multivariant least square fit to the density profiles derived from the RPI sounding measurements.

[25] Along the nightside outbound and dayside inbound orbit segments on 21–22 February 2001, the IMAGE RPI obtained a number of plasmagrams containing distinct traces that can be used to derive the field-aligned density profiles with the inversion technique described by *Huang et al.* [2004]. The derived field-aligned density profiles on the nightside and dayside are shown in Figures 6a and 6b, respectively (solid lines). The times and L shells of the measurements for those density profiles are listed in Table 1. As mentioned previously, IMAGE encountered the nightside plasmapause at ~1436 UT on 21 February 2001 and the dayside plasmapause at ~0206 UT on the next day. The times of the measurements indicate that profiles 1–2 and profiles 3–7 were measured in the nightside plasmasphere and plasmatrough, respectively. The dayside profiles 8–10 were measured in the dayside plasmatrough. It is seen from Figure 6 that these three groups of density profiles have very different slopes. Therefore, the multivariant least squares fit of equation (1) is applied separately to these three groups of density profiles. The obtained three sets of values for the fitting parameters A, B, C, and D, along with the equatorial density N_{eq} for each individual density profile that is obtained by extrapolating the fitting density profile to the equator, are listed in Table 1. The fitted density profiles are superimposed on the measured density profiles in Figures 6a and 6b (dotted lines). It can be seen that the measured density profiles are well modeled by equation (1) (the relative differences between the modeled and measured densities are less than 10%). Figures 6c and 6d show the extrapolated equatorial electron density N_{eq} as a function of L shell for the nightside and dayside region, respectively. The equatorial densities are labeled with the same number as the corresponding density profiles. The equatorial densities in the dayside plasmatrough (Figure 6d) are slightly higher than those in the nightside plasmatrough (Figure 6c) at the same L values, indicating that there really exists plasma refilling along the flux tubes originating in the nightside plasmatrough. It is noted that the equatorial densities are not directly measured but extrapolated from the fitting density profiles. *Tu et al.* [2006] have shown that such extrapolation is reasonable because the extrapolation is constrained by the trend of the multiple density profiles measured by the IMAGE RPI.

[26] With the variations of the equatorial density, it is possible to estimate the refilling rate for a given flux tube in the plasmatrough for this event. Since the field-aligned density profiles in the dayside plasmasphere were not available, we are unable to estimate the refilling rates for the flux tubes in the dayside plasmasphere region. We chose a flux tube near the geosynchronous orbit on the nightside and traced it to the dayside, where it arrives near the projection of IMAGE on the equatorial plane. The starting location of the flux tube is in the IMAGE orbit plane on the nightside. The tracing results are exhibited in Figures 5e and 5f in the same format as that of Figures 5a and 5b. As can be seen, at the starting time (1452 UT on 21 February) the flux tube is located in the nightside plasmatrough at L = 6.4, a location near the geosynchronous orbit, while at the ending time (0152 UT on 22 February) it has drifted slightly outward to L = 7.0 (Figure 5f, rectangle) in the dayside plasmatrough. The L shell change of this tracing from nighttime to daytime is also marked in Figure 3c as a curved arrow, from the vertical dashed line to the vertical solid line. The interpolated equatorial densities of the flux tube at L = 6.4 in the nighttime and L = 7.0 in the daytime thus are 2.3 and 5.0 cm^{-3}, respectively. They are labeled as solid circles in Figures 6c and 6d. Note that the stating equatorial location of the flux tube traced is in the IMAGE orbit plane, and the ending equatorial location of the flux tube is close to the IMAGE orbit plane. Therefore, it is reasonable to assume that the interpolated equatorial densities roughly represent the equatorial densities at the starting and ending locations of the flux tube, respectively.

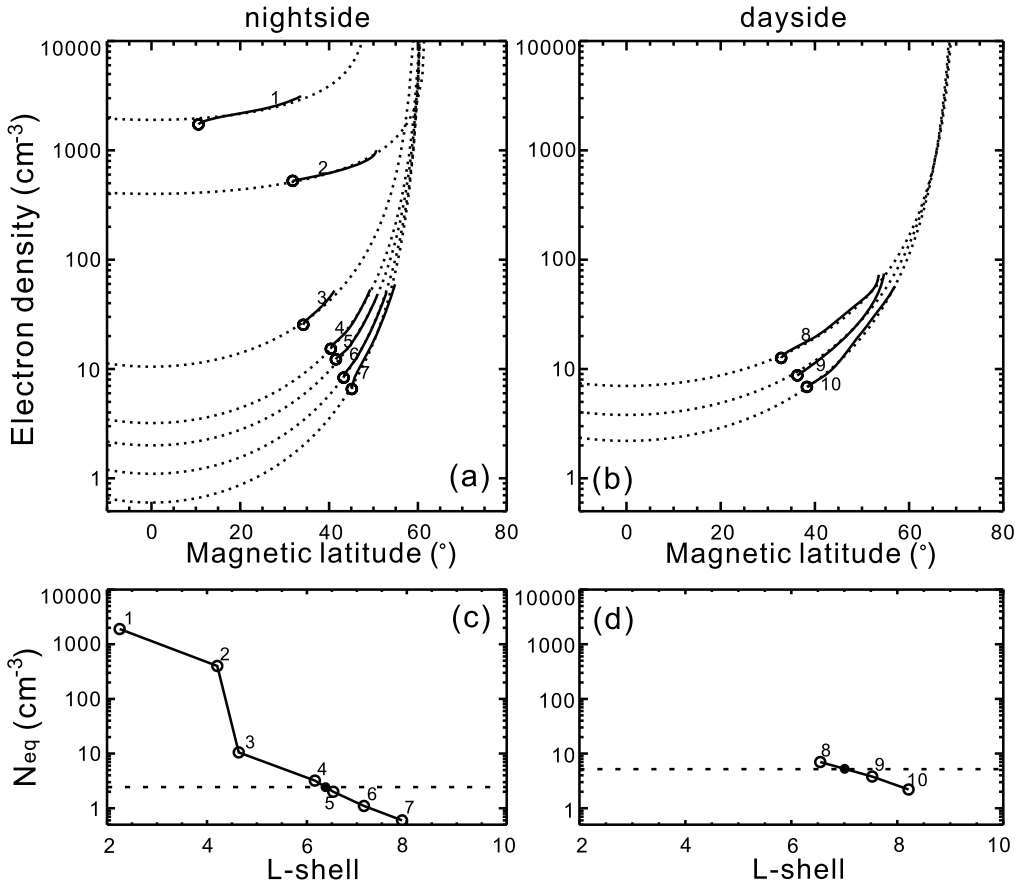

Figure 6. (a, b) Field-aligned electron density profiles derived from the RPI active sounding measurements (solid lines) on (a) the nightside and (b) the dayside in the interval of 21–22 February 2001. The dotted lines denote the fitted profiles. (c, d) The equatorial density deduced from the multivariant least squares fitting of equation (1) to the measured density profiles. Open circles in Figures 6a and 6b and in Figures 6c and 6d indicate the in situ electron densities observed by the RPI and the derived equatorial densities, respectively. The solid circle in Figures 6c and 6d represents the equatorial density of a traced flux tube at its initial and final locations, respectively. See text for details.

3.1.4. Defense Meteorological Satellite Program Observations of Refilling Sources

[27] We have examined the available DMSP satellite observations to see if there is plasma supply from the ionosphere to the high altitudes, that is, to ensure that there are indeed refilling processes as we suggested above. Figure 7 presents the measurements by DMSP F15 in the interval of 1908–2050 UT on 21 February 2001. Because the drift path of the flux tube shown in Figure 5f passes the DMSP F15 orbit segment in the early morning local time (~0900 MLT) at about 1900 UT, we consider that the DMSP 15 satellite roughly encountered the traced flux tube. Figure 7 shows the number densities of the total ion (Figure 7a) and H^+ (Figure 7b), the total ion velocity parallel to the magnetic field line $V_{\|}$ (Figure 7c), the total ion flux (Figure 7d) and the H^+ flux (Figure 7e). The number densities in Figures 7a and 7b were measured by the RPA instrument. The parallel velocity $V_{\|}$ is deduced from the horizontal velocities V_x and V_y and the vertical velocity V_z assuming that the geomagnetic field is a dipole field at the altitude of

Table 1. Values of Fitting Parameters A, B, C, D, and N_{eq} for the Nightside Plasmasphere, Nightside Plasmatrough, and Dayside Plasmatrough[a]

	Profile	UT	L Shell	N_{eq}	A	B	C	D
NPS	1	1411:10	2.25	1900	0.98	0	0.45	0.055
	2	1435:10	4.21	400				
NPT	3	1439:10	4.64	10.5	0.91	0.027	0.99	0.22
	4	1451:34	6.20	3.2				
	5	1454:16	6.53	2.0				
	6	1458:34	7.14	1.1				
	7	1503:34	7.90	0.6				
DPT	8	0159:08	6.55	7.0	0.80	0.023	0.20	0.30
	9	0148:10	7.53	3.8				
	10	0141:11	8.21	2.2				

[a]Profile numbers are associated with those in Figure 6. The equatorial densities N_{eq} are in cm^{-3}. Abbreviations are as follows: DPT, dayside plasmatrough; NPS, nightside plasmasphere; NPT, nightside plasmatrough.

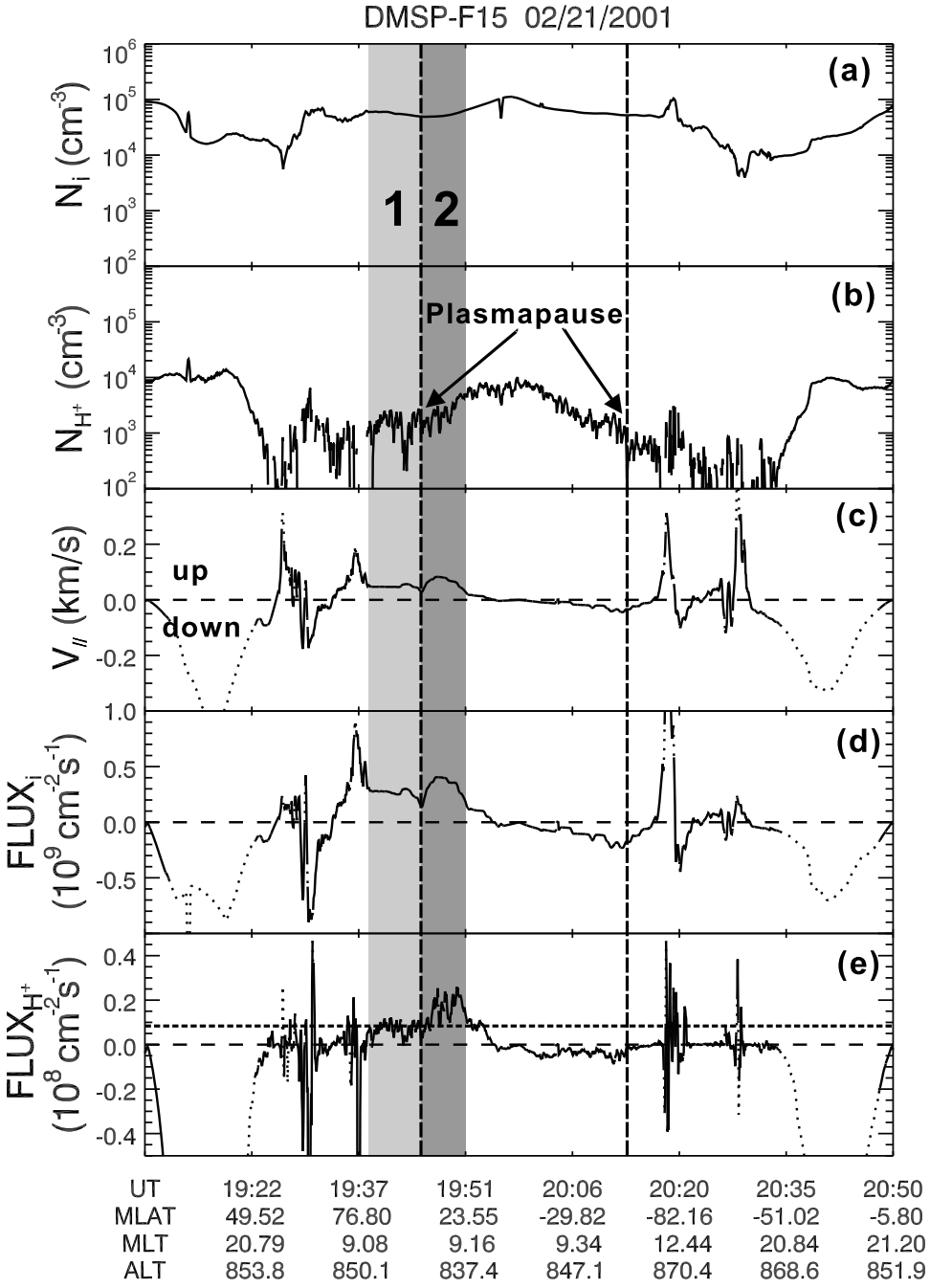

Figure 7. Plasma parameters measured by Defense Meteorological Satellite Program (DMSP) F15 from 1908 to 2050 UT on 21 February 2001. (a) Number density of the total ions from the retarding potential analyzer (RPA). (b) Number density of H^+ from the RPA. (c) Derived ion velocity along the geomagnetic field line. (d) Derived ion density flux along the field line. (e) Derived H^+ density flux along the field line. The two vertical dash lines indicate the inner boundary of the light ion trough, which is also consistent with the mapping of the location of the plasmapause along the magnetic field line. Shaded regions 1 and 2 represent, respectively, the plasmatrough and the outer plasmasphere in the local time around 9000 MLT. The data represented by solid lines in Figures 7c–7e are reliable, while that the data represented by the dotted lines are unreliable.

DMSP, where V_x is in the direction along the spacecraft orbit, V_y is in the cross-track direction, and V_z points outward from the center of Earth. A positive $V_{||}$ represents a field-aligned upward flow, which in turn refills the plasmasphere and trough. The solid lines in Figure 7 indicate that the data are reliable, while the dotted lines in Figure 7 indicate that they are unreliable. The orbit information is labeled below the abscissa. The low number density of H^+ in the plasmatrough corresponds to the light ion trough (LIT) in the topside ionosphere [*Lemaire*, 2001; *Anderson et al.,* 2008]. The larger

density and fluxes of heavy ions observed in the ionosphere may have little effect on the refilling in the equatorial region because, due to their heavier masses and slower speeds, they may not be able to escape from the gravity and they fall back to the ionosphere. The vertical dashed lines in Figure 7 indicate the inner boundary of those LITs, which thus corresponds to the plasmapause at high altitude. It should be pointed out that the plasmapause observed by DMSP at $L = \sim 4.6$ agrees well with that predicted by the E5D electric model at $L = \sim 4.8$, indicting that the E5D model used in this study is reasonable. Between the two vertical lines in Figure 7 is the plasmasphere. In the time period shown, the light ion trough of low density was observed twice: one above the Northern Hemisphere and the other above the Southern Hemisphere (see the low-density region of H^+ in Figure 7b). It is seen that there are upward flows along the magnetic field lines in the shaded regions 1 and 2, which correspond to the plasmatrough and outer plasmasphere, respectively, at the local time around 0900 MLT (see Figure 7c). Note that toward the high latitudes the peak upward velocity is associated with the typical larger upward flows in the aurora zone.

[28] In Figure 7c, the upward velocity in the plasmatrough is ~50 m s^{-1} (shaded region 1). The associated upward total ion and H^+ density flux are ~2.7×10^8 and ~8.0×10^6 cm^{-2} s^{-1} (see Figures 7d and 7e), respectively. The upward velocity is higher in the outer plasmasphere and can reach ~90 m s^{-1} (Figure 7, shaded region 2), about twice as large as that in the plasmatrough. The upward fluxes of the total ion and H^+ in the outer plasmasphere are ~4.0×10^8 and ~2.4×10^7 cm^{-2} s^{-1}, respectively. Here we pay more attention to the upward flux of H^+ since the ions that can reach the high-altitude plasmasphere along the magnetic field lines are primarily the light ions. Most of the heavy ions such as O^+ are bounded by gravity to lower altitudes. It is seen that the upward flux of H^+ in the outer plasmasphere is about 3 times as large as that in the plasmatrough. The upward H^+ fluxes observed by the DMSP F15 indicate that there is plasma supply from the ionosphere to the plasmasphere and plasmatrough. The much larger upward flux in the outer plasmasphere implies a larger refilling rate there compared to the plasmatrough. This is consistent with the RPI observations of the larger density increase from the density level of the nightside plasmatrough to form the outer plasmasphere on the dayside (see Figure 3). It is worth noting that the field-aligned flow in the Northern Hemisphere is upward, while it is downward in the Southern Hemisphere, indicating an interhemispheric flow from the Northern Hemisphere to the Southern Hemisphere.

3.1.5. Refilling Rate Near the Geosynchronous Orbit

[29] We now estimate the refilling rate in the traced flux tube near the geosynchronous orbit. The DMSP F13 satellite, which circles Earth from dusk to dawn, provides complementary observations for determining the time when the refilling begins. Because DMSP F13 did not observe significant upward flux (not shown here) when it passed the dawn sector, about 0600 MLT, during this event, the refilling should not start before ~1602 UT on 21 February. If the refilling ended before ~0152 UT when the higher densities were observed on the dayside by IMAGE on 22 February, the refilling time period is about or less than 9.8 h. Considering that the equatorial densities at initial and ending times are 2.3 and 5.0 cm^{-3}, respectively, the refilling rate is thus calculated to be ~0.27 cm^{-3} h^{-1}. This rate is within but at the lower end of the range of 0.21–0.54 cm^{-3} h^{-1} as given by *Su et al.* [2001] for the early time refilling. The relatively small refilling rate may be the reason that the density in the dayside plasmatrough is not elevated to the level of that inside the dayside plasmasphere but remains as low as that in the nightside plasmatrough.

3.1.6. Geomagnetic Condition

[30] We examine the effects of the geomagnetic activities and solar wind/IMF conditions. In Figure 4, the two vertical lines denote the interval between the IMAGE RPI observations on the nightside and dayside. We see that during that interval the IMF B_z was primarily northward with some fluctuations, and the ram pressure of the solar wind was low and nearly constant. The geomagnetic condition was quiet, as indicated by the D_{st} and K_p indices. Note that in the interval between the RPI observations on the nightside and dayside, the K_p index was below 2 and in general decreasing. The magnetospheric convection during that period was expected to be weak and possibly further decreased. This may explain why the flux tubes previously on the open drift paths in the nightside trough find them on the closed drift paths on the dayside as demonstrated by the drift trajectory shown in Figures 5c and 5d. We therefore conclude that the outward relocation of the plasmapause when the plasmasphere rotated from the nightside to the dayside was caused by the refilling combined with the decreased convection.

3.2. Case of 28 August 2005

[31] The above observations show a case in which the well-defined plasmapause on the nightside relocated outward on the dayside. We now present a case with a very different morphology, which was observed on 28 August 2005 when the inner magnetosphere was recovering from a magnetic storm that occurred on August 24.

[32] Figure 8 displays the dynamic spectra from the passive measurements of the RPI for the outbound orbit segment from 0200 to 0500 UT on 28 August 2005 (nightside) and for the inbound orbit segment from 1400 to 1700 UT (dayside). The UHR band is clearly visible, and there is a sudden change in its frequencies at ~0352 UT, indicating that IMAGE passed the plasmapause at that time. The frequency variation of the UHR band along the inbound orbit is quite smooth, giving no indication of an abrupt plasmapause. Figure 9 presents the electron densities derived from the lower cutoff frequencies of the UHR bands. IMAGE observed an electron density change from 100 to 10 cm^{-3} at $L = \sim 4.5$ and at ~0352 UT, a clearly defined plasmapause on the nightside. However, in the dayside region (Figure 9b), the electron density decreases smoothly from 2830 to 5 cm^{-3} without an identifiable plasmapause. This phenomenon is even more obvious when the density distributions are plotted as a function of L shell (Figure 9c). The electron density in the dayside inner magnetosphere is one order of magnitude higher than that in the nightside plasmatrough.

[33] We now examine the geomagnetic conditions for this case, which are shown in Figure 10. Similar to the case discussed in the previous section, the RPI observations were made during a geomagnetic quiet period in terms of K_p indices. The difference from the previous case is that this case was in the recovery phase of a magnetic storm, as shown by the inset, which displays the variation of the D_{st} index from

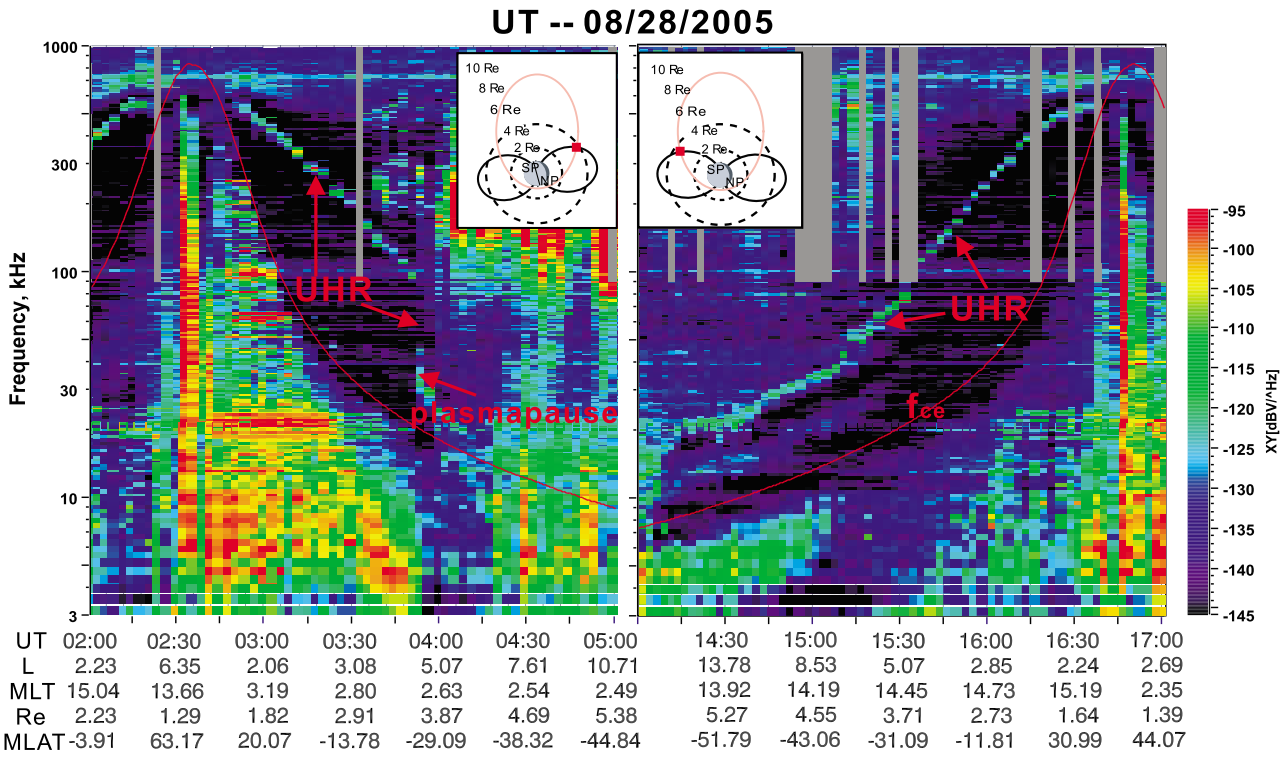

Figure 8. The dynamic spectra in the same format as in Figure 2 but for the case of 28 August 2005. A distinct plasmapause on the nightside becomes a gradually changed density distribution in daytime, as shown in Figure 8 (right).

23 to 29 August 2005. This magnetic storm led to a drop of the D_{st} index from 0 to less than −200 nT. During the interval of the RPI observations, the K_p values were at or below 1 and relatively steady. The IMF B_z was primarily northward, and the ram pressure of the solar wind was about 1 nPa and steady. Since the geomagnetic conditions were quiet and steady at the time, it is not expected that the flux tubes inside the nightside plasmapause move significantly outward to cause the high densities observed by the RPI on the dayside at larger L shells beyond the location corresponding to the nightside plasmapause (at L = ~4.5). In other words, the smooth density distribution on the dayside is most likely a consequence of the refilling of the flux tubes originating in the nightside plasmatrough. We further investigate this possibility by tracing flux tubes originating from the nightside plasmatrough to the dayside.

[34] The drift trajectory of a sample flux tube in the nightside plasmatrough is traced using the E5D and T96 models. The tracing of the flux tube trajectory starts at 0415 UT on 28 August 2005, at L = 6.2 and 0234 MLT, where and when IMAGE passed the flux tube. The initial location of the flux tube in the SM equatorial plane is displayed in Figure 11a as a triangle with the electric equipotential lines at that time. The flux tube is in the region of open drift paths. The flux tube is traced until 1509 UT of 28 August 2005, at L = 7.3 and 1414 MLT. The ending location (indicated by a square in Figure 11b) is again chosen to make it closest to the IMAGE orbit projection on the equatorial plane. The ending location of the flux tube is also on the open drift paths, as demonstrated by the equipotential lines on the snapshot at 1509 UT. Since after tracing for more than 0.5 day the model location is close to the IMAGE orbit projection, it is reasonable to conclude that the flux tubes encountered by IMAGE on the dayside inner magnetosphere most likely came from the nightside plasmatrough. Thus the higher density seen by IMAGE compared to the nightside plasmatrough density is most likely due to the fast refilling of the flux tubes along the field lines.

[35] In order to estimate the refilling rate for the flux tube traced, we first derive the equatorial density variations, again, with the field-aligned density profiles derived from the RPI sounding measurements. In the present case, good-quality traces that can be used to derive the field-aligned density distributions are only available in the nightside plasmatrough and in the dayside large-L shell region. The times and L values of the measurements of those field-aligned density profiles are listed in Table 2. The density profiles on the nightside and dayside are plotted in Figures 12a and 12b, respectively. Multivariant least square fits with equation (1), separately for the nightside and dayside groups of the density profiles, extrapolate the equatorial densities as plotted in Figures 12c and 12d for the nightside and dayside and listed in Table 2. The fitting density profiles are displayed as the dotted lines in the Figures 12a and 12b. Note that the equatorial densities in the dayside, even at larger L values, are higher than those in the nightside plasmatrough. The extrapolated equatorial density of the traced flux tube at its initial location is inferred to be 1.1 cm^{-3}, as the solid circle shown in Figure 12c, while it is 10.2 cm^{-3} at its final location, as the solid circle shown in Figure 12d.

[36] The stronger refilling in the present case is also supported by the DMSP F15 observations, which are shown

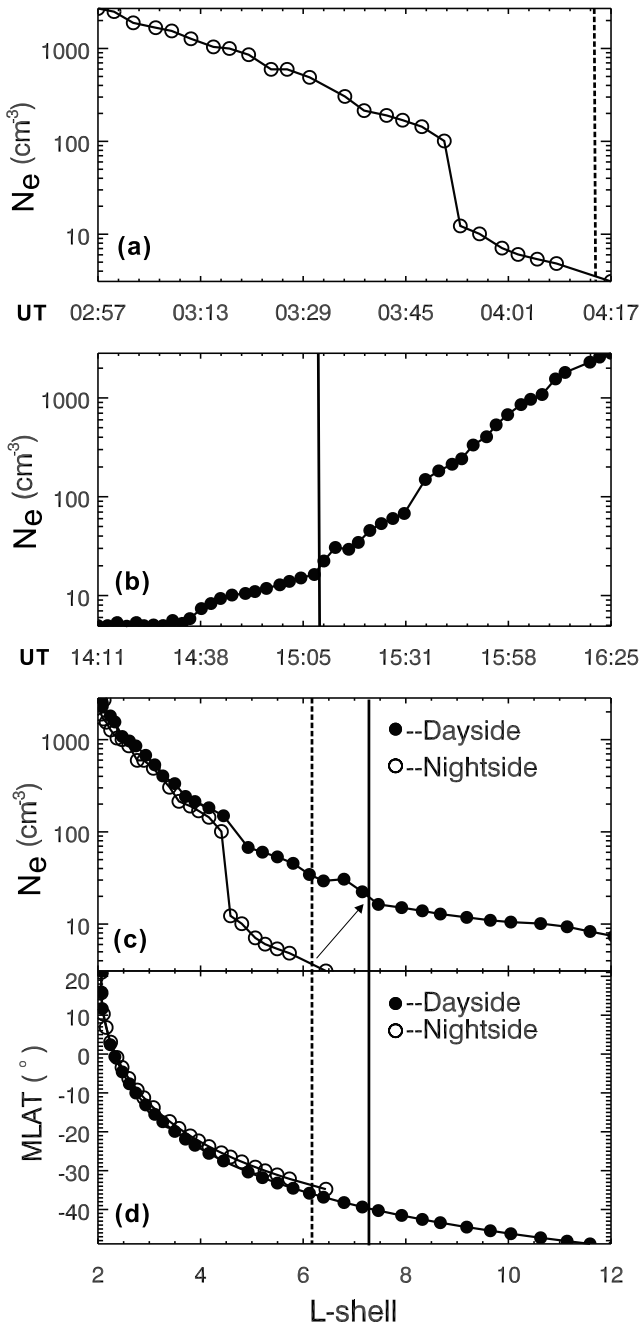

Figure 9. The derived plasma densities in the same format as in Figure 3 but for the electron density distributions in the 28 August 2005 case. The vertical dotted lines indicate the initial time and L shell of a flux tube, and the solid lines indicate its final time and location after it drifts from the nightside to the dayside. The arrow in Figure 9c indicates the moving direction of the flux tube in the L shell.

in Figure 13 in the same format as Figure 7. As indicated by the shaded region in the figure, a large upward velocity in excess of 250 m s^{-1} was observed (Figure 13c) in the Northern Hemisphere in the prenoon region when the DMSP satellite was located beyond the plasmapause that can be recognized by the LIT in Figure 13b. The derived total ion density flux (Figure 13d) and H^+ density flux (Figure 13e) are ~7.0×10^8 and ~2.0×10^7 cm^{-2} s^{-1}, respectively. They are much larger than those in the 21–22 February 2001 case. Obviously these upward fluxes occurred in a large range of L shells, in a good agreement with the RPI observations shown in Figure 9c, where the region of the elevated densities on the dayside extends from L = 4.5 up to L > 12. There is almost no upward flux inside the plasmapause, outside of the shaded area in Figure 13.

[37] We also examined the observations by the DMSP F13 and F14 satellites, and we found no significant upward flux of the ionospheric ions on the dawnside (data not shown), suggesting that the refilling started after the traced flux tube passed the dawn terminator, corresponding to a refilling start time after 0452 UT. The refilling time period is thus from after 0452 UT to 1509 UT, that is, less than 10.3 h, translating into a refilling rate greater than 0.88 cm^{-3} h^{-1}. This refilling rate is much larger than that derived in the previous case for the flux tube that started at similar L shell (L = 6.4).

[38] We now examine whether this large refilling rate derived from RPI can be explained by the upward flux observed by DMSP 15. Here, we again look at only light ions. Assuming the electron density distribution in the flux tube can be expressed by the density profile derived from the RPI sounding measurements (see Figure 12), the total number of the electrons (from the DMSP altitude to the equator) in the tube with an area of 1 m^{-2} at the DMSP altitude can be estimated by integration along the flux tube. In the present case, the total number of the electrons in the traced flux tube on the nightside is estimated to be ~2.12×10^{15}, while the total number of the electrons in the traced flux tube on the dayside is ~1.10×10^{16}. The difference is ~8.89×10^{15} electrons, which is the required amount of the electrons to refill the traced flux tube. From the DMSP F15 observations (Figure 13), we can estimate the total number of supplied H^+ ions to be ~7.42×10^{15} from 0452 to 1509 UT, assuming that the upward H^+ flux remained constant during the refilling period. The supplied amount of H^+ is thus comparable to the required amount if we assume that the H^+ ion density is basically the electron density in the plasmasphere. This would indicate that the flux originating from the ionosphere may be the source of the density increase from the nighttime to the daytime. We may now conclude that the extended region of elevated densities on the dayside as seen in Figure 9 was due to the stronger refilling extending to the larger L shells.

[39] It is interesting to review the refilling rates near the geostationary orbit obtained from the previous observations and simulations to see whether the refilling rates derived from the present observations stand. We indicate that in the present study we observed the early time refilling because the nearly empty flux tube experienced its first pass of the dayside [*Gallagher et al.*, 1998; *Lawrence et al.*, 1999; *Su et al.*, 2001]. The early time refilling rates near the geostationary orbit obtained from a number of previous observations and simulations, along with those derived from the present observations, are listed in Table 3. It is seen that the refilling rates derived here are within the range of the rates obtained in previous studies, especially the range of the rates from the observations. For the case of the typical evolution, the rate is within but at the lower end of the range of 0.21–0.54 cm^{-3} h^{-1}

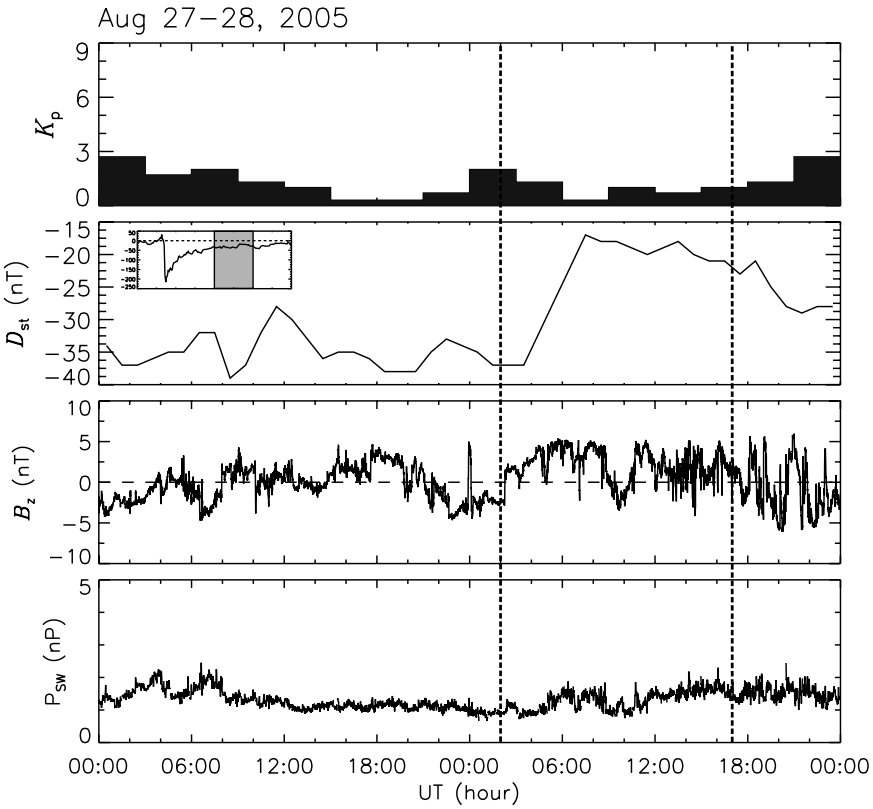

Figure 10. The geomagnetic indices and solar wind conditions in the same format as in Figure 4 but on 27–28 August 2005. The inset displays a magnetic storm that occurred on August 24 2005. The two vertical dotted lines roughly indicate the time interval of the IMAGE RPI observations made on the nightside and the dayside.

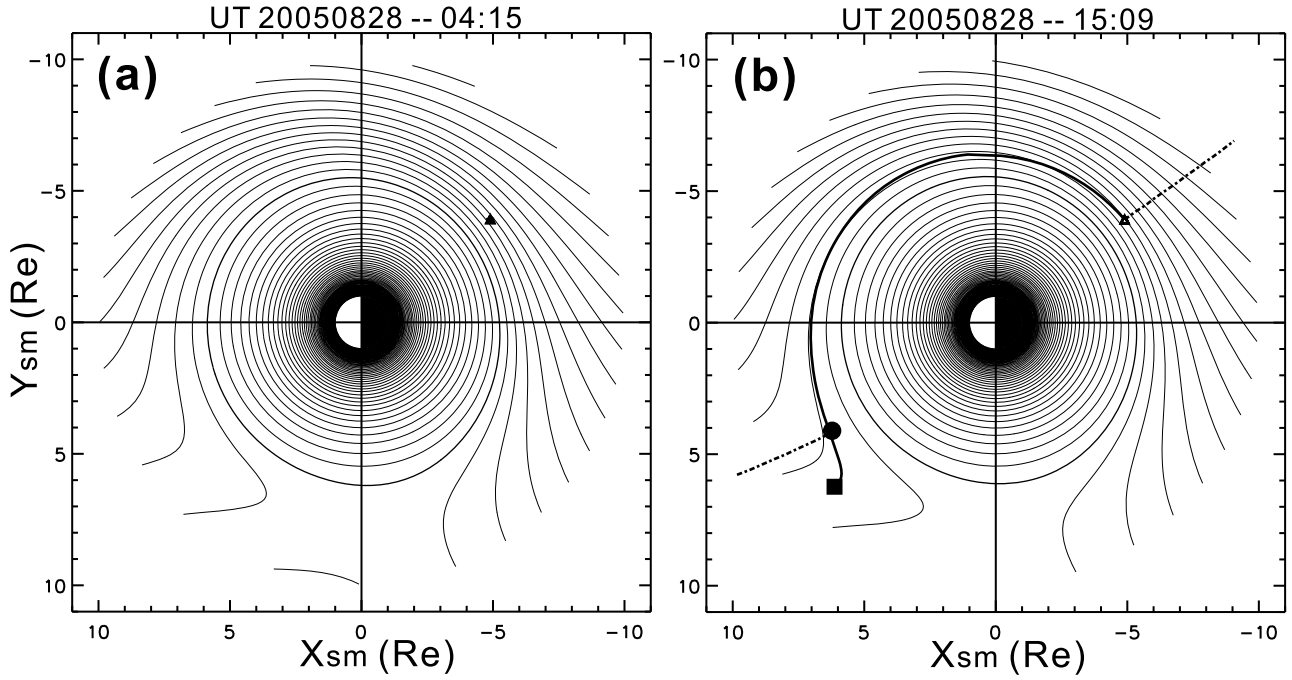

Figure 11. Drift trajectory tracing in the same format as in Figure 5 but for a flux tube located initially at L = 6.2 and 2.57 MLT. The tracing starts at 0415 UT and ends at 1509 UT on 28 August 2005.

Table 2. Values of Fitting Parameters A, B, C, D, and N_{eq} for the Nightside Plasmasphere and Dayside Inner Magnetosphere for the 28 August 2005 Case[a]

	Profile	UT	L shell	N_{eq}	A	B	C	D
NPT	1	0353:21	4.57	4.7	0.99	0.061	0.60	0.12
	2	0402:22	5.25	3.0				
	3	0405:04	5.46	2.4				
DIM	4	1507:40	7.51	9.0	0.99	0.009	0.45	0.10
	5	1505:27	7.79	8.0				
	6	1501:22	8.34	5.8				

[a]Profile numbers are associated with those in Figure 12. The dayside inner magnetosphere is given since no plasmatrough exists in daytime for this case. The equatorial densities N_{eq} are in cm^{-3}. Abbreviations are as follows: DIM, dayside inner magnetosphere; NPT, nightside plasmatrough.

given by *Su et al.* [2001]. For the fast refilling case, on the other hand, the rate is within but at the upper end of the range of 0.05–1.0 cm^{-3} h^{-1} given by *Lawrence et al.* [1999].

4. Summary and Discussions

[40] In the present study, we have investigated two cases of the evolution of the inner magnetosphere from the nighttime to the daytime by analyzing both the passive and active measurements from IMAGE RPI. Both cases were observed under quiet geomagnetic conditions in terms of K_p indices. The difference is that the second one was observed during a recovery phase of a magnetic storm. In the first case the well-defined plasmapause on the nightside persisted on the dayside when the plasmasphere corotated with Earth but the location of the plasmapause moved outward. This is the typical evolution of the inner magnetosphere as normally expected. In the second case the plasma density in the entire plasmatrough was significantly elevated when the flux tubes in the nightside plasmatrough had drifted to the dayside. There is no identifiable plasmapause. By tracing the drifts of the flux tubes initially in the nightside plasmatrough, we showed that such plasmaspheric density distribution evolution could not be formed by simple convection and corotation of the inner magnetosphere. The fast refilling along the field from the ionosphere has to be invoked. The DMSP F15 observations provide supporting evidence that the evolution of the inner magnetosphere from the nightside to the dayside is primarily controlled by the refilling processes with greater upward fluxes in the region of elevated densities, which in the second case extends to at least $L = 10$. The present study demonstrates the importance of the plasmasphere-ionosphere coupling in controlling the structures of the inner magnetosphere.

[41] It should be pointed that the absence of the plasmapause on the dayside is not correlated with a plasmasphere plume because when a satellite crosses a plume structure, at least one plasmapause-like boundary (the outmost), and

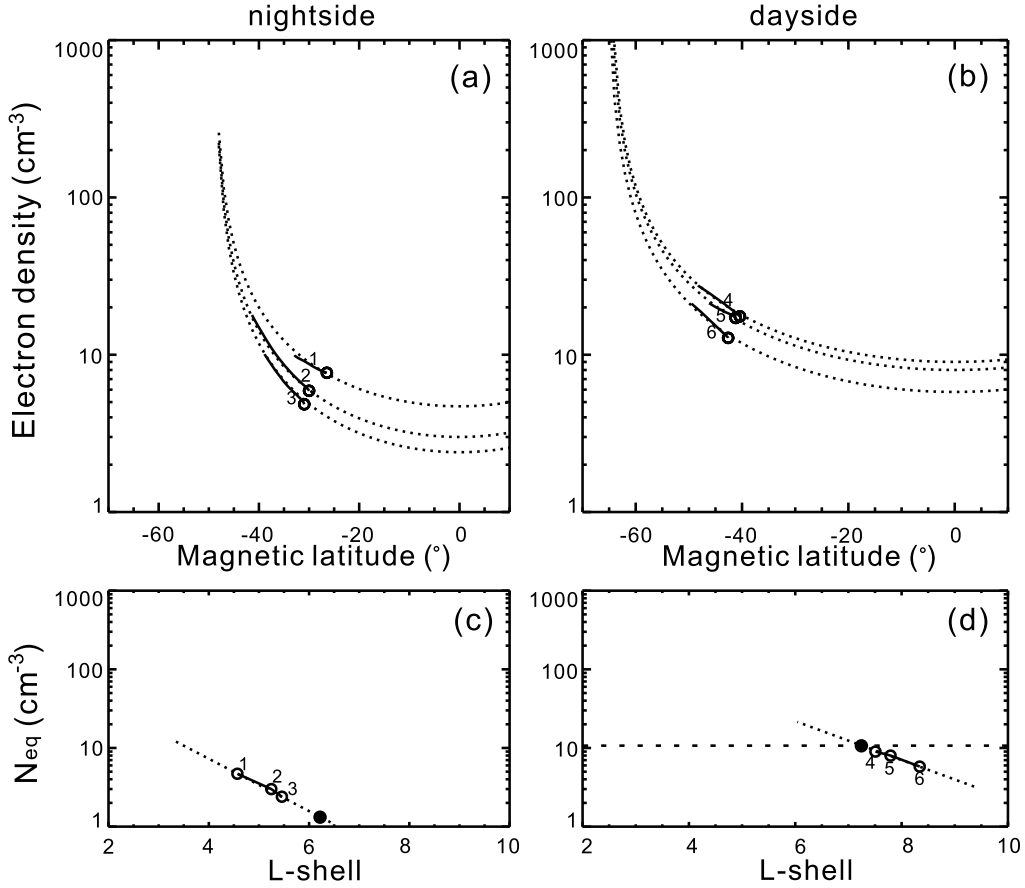

Figure 12. The electron density profiles along the magnetic field in the same format as in Figure 6 but for the 28 August 2005 case. The dotted lines in Figures 12c and 12d are drawn as a reference.

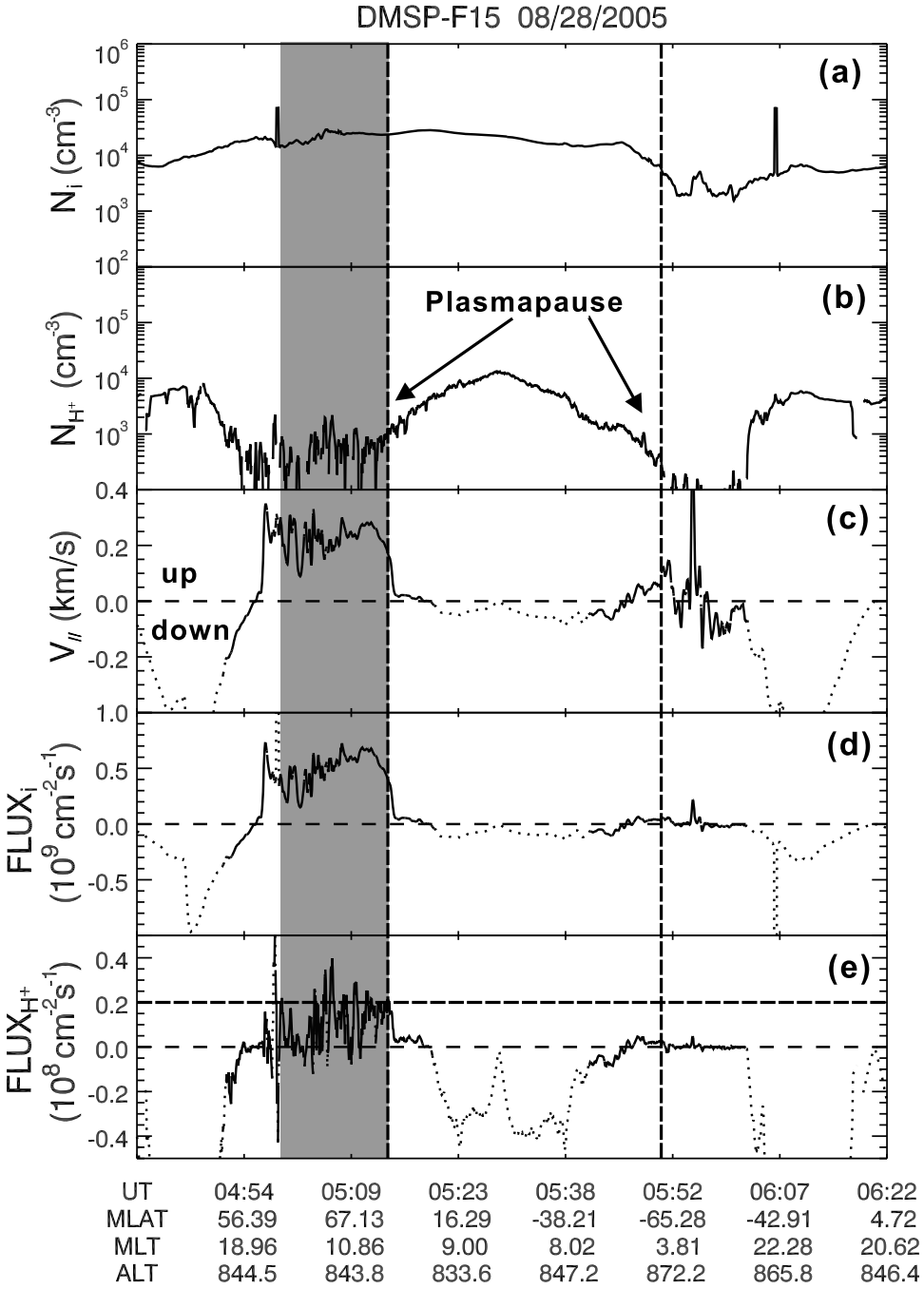

Figure 13. The DMSP observations in the same format as in Figure 7 but for the period 0440–0622 UT on 28 August 2005. The solid lines indicate data that are reliable, and the dotted lines indicate data that are unreliable.

sometimes three boundaries, should be observed. This is not true in the second case we presented, in which no density boundary is observed even up to $L > 12$. In addition, the plume is usually considered to exist in the region $L < 10$ and under disturbed geomagnetic conditions in terms of $K_p > 3$ [*Darrouzet et al.*, 2008], inconsistent with the very low K_p situation ($K_p < 1$) in the second case. We also examine the global images of the plasmasphere taken by the Extreme Ultraviolet Imager [*Sandel et al.*, 2000] on board the IMAGE satellite. There are no plasmasphere plumes observed on that day.

[42] By using the field-aligned density profiles derived from the RPI remote sounding measurements and tracing the drifts of the flux tubes, we have estimated the early stage refilling rate for the flux tubes originating from the nightside plasmatrough. Although the estimate of the refilling rate is subject to some uncertainties due to the models for the magnetospheric electric and magnetic fields and the

Table 3. Early Time Refilling Rates Near the Geosynchronous Orbit[a]

Contributor	Satellite/Model	Plasma Species	Refilling Rate (cm^{-3} h^{-1})
Higel and Wu [1984]	GEOS 2	Total electron density	0.66
Carpenter and Anderson [1992]	ISEE/Whistler	Total electron density	0.287
Gallagher et al. [1998]	GEOS 2	Total electron density	0.56
Lawrence et al. [1999]	LANL MPA	Low-energy (≤100 eV) ions	0.05–1.0
Su et al. [2001]	LANL MPA	Low-energy (≤100 eV) ions	0.21– 0.54
Singh et al. [1986]	Single-stream model	H^+ density	1.5
Wilson et al. [1992]	Semikinetic model	H^+ density	0.75
Present study (typical evolution)	IMAGE RPI	Total electron density	>0.27
Present study (fast refilling)	IMAGE RPI	Total electron density	>0.88

[a]The rates expressed in cm^{-3} d^{-1} have been converted to cm^{-3} h^{-1} by assuming 12 h refilling for a day. Abbreviations are as follows: IMAGE, Imager for Magnetopause-to-Aurora Global Exploration; LANL, Los Alamos National Laboratory, Los Alamos, New Mexico; MPA, Magnetospheric Plasma Analyzer; RPI, Radio Plasma Imager.

extrapolation of the field-aligned density to the equator, the values for the refilling rates derived in the present study are consistent with those obtained in previous observations [e.g., *Lawrence et al.*, 1999; *Su et al.*, 2001] at similar L shell. The refilling rate for the flux tubes reaching the dayside plasmatrough in the two cases is at the lower and upper ends, respectively, of the range of the refilling rates obtained by the previous observations. This indicates that the refilling rates estimated in the present study are reasonable. The larger region of the fast refilling in the second case is also consistent with the fact that the DMSP F15 observed a larger region of the upward H^+ ion fluxes.

[43] It is necessary to state that the electric model we employed to trace the motion of the flux tubes from nighttime to daytime, that is, the E5D model, appears to work very well in this study. In the first case, the L shell of the plasmapause predicted by the E5D model is almost the same as that observed by the IMAGE RPI on both the nightside and the dayside and is also the same as the DMSP observation in the postdawn sector in the ionosphere.

[44] In the cases presented the geomagnetic activities in terms of K_p index were quiet. It is very interesting that the fast refilling region is confined (inside L = ~6.3) in the first case but extended to much larger L shells in the second case. This difference may be due to the significantly different geomagnetic conditions of the two cases. In the second case, the refilling was observed during the recovery phase of a magnetic storm. During the storm, the energy input to the ionosphere increased, leading to enhanced electron and ion temperatures. The consequences are the raised plasma scale height and increased parallel (bipolar in nature) electric field so as to increase upward plasma flux. These effects may persist during the recovery phase of the magnetic storm. At magnetospheric altitudes there may be enhanced wave-particle interaction and hot-cold ion interaction, favoring the fast refilling in the extended region of the inner magnetosphere. Further investigations are needed in order to provide full explanation for the observations.

[45] **Acknowledgments.** This work was supported by NASA grants NNX07AG38G and NNX08AF31G, NSF grant ATM-0902965 to the University of Massachusetts, Lowell, National Basic Research Program of China grants 2006CB806305 and 40523006, and the Specialized Research Fund for Chinese State Key Laboratories. We gratefully acknowledge the Center for Space Sciences at the University of Texas at Dallas and the U.S. Air Force for providing the DMSP thermal plasma data.

[46] Zuyin Pu thanks Nagendra Singh and another reviewer for their assistance in evaluating this manuscript.

References

Anderson, P. C., W. R. Johnston, and J. Goldstein (2008), Observations of the ionospheric projection of the plasmapause, *Geophys. Res. Lett.*, *35*, L15110, doi:10.1029/2008GL033978.

Benson, R. F., P. A. Webb, J. L. Green, L. Garcia, and B. W. Reinisch (2004), Magnetospheric electron densities inferred from upper-hybrid band emissions, *Geophys. Res. Lett.*, *31*, L20803, doi:10.1029/2004GL020847.

Burch, J. L. et al. (2001), Views of Earth's magnetosphere with the IMAGE satellite, *Science*, *91*(5504), 619–624, doi:10.1126/science.291.5504.619.

Carpenter, D. L. (1963), Whistler evidence of a "knee" in the magnetospheric ionization density profile, *J. Geophys. Res.*, *68*(6), 1675–1682, doi:10.1029/JZ068i006p01675.

Carpenter, D. L., and R. R. Anderson (1992), An ISEE/Whistler model of equatorial electron density in the magnetosphere, *J. Geophys. Res.*, *97*(A2), 1097–1108, doi:10.1029/91JA01548.

Carpenter, D. L., and J. Lemaire (1997), Erosion and recovery of the plasmasphere in the plasmapause region, *Space Sci. Rev.*, *80*, 153–179, doi:10.1023/A:1004981919827.

Carpenter, D. L., and J. Lemaire (2004), The plasmasphere boundary layer, *Ann. Geophys.*, *22*, 4291–4298.

Darrouzet, F., J. De Keyser, P. M. E. Décréau, F. El Lemdani-Mazouz, and X. Vallières (2008), Statistical analysis of plasmaspheric plumes with Cluster/WHISPER observations, *Ann. Geophys.*, *26*, 2403–2417.

Frank, L. A. (1971), Relationship of the plasma sheet, ring current, trapping boundary, and plasmapause near the magnetic equator and local midnight, *J. Geophys. Res.*, *76*(10), 2265–2275, doi:10.1029/JA076i010p02265.

Fu, H. S., J. Tu, J. B. Cao, P. Song, B. W. Reinisch, D. L. Gallagher, and B. Yang (2010), IMAGE and DMSP observations of a density trough inside the plasmasphere, *J. Geophys. Res.*, doi:10.1029/2009JA015104, in press.

Fung, S. F., and J. L. Green (2005), Modeling of field-aligned guided echoes in the plasmasphere, *J. Geophys. Res.*, *110*, A01210, doi:10.1029/2004JA010658.

Galkin, I., B. Reinisch, G. Grinstein, G. Khmyrov, A. Kozlov, X. Huang, and S. Fung (2004), Automated exploration of the Radio Plasma Imager data, *J. Geophys. Res.*, *109*, A12210, doi:10.1029/2004JA010439.

Gallagher, D. L., P. D. Craven, and R. H. Comfort (1998), A simple model of magnetospheric trough total density, *J. Geophys. Res.*, *103*(A5), 9293–9297, doi:10.1029/97JA03665.

Green, J. L., and B. W. Reinisch (2003), An overview of results from RPI on IMAGE, *Space Sci. Rev.*, *109*, 183–210, doi:10.1023/B:SPAC.0000007519.44362.65.

Hairston, M. R., and R. A. Heelis (1990), Model of the high-latitude ionospheric convection pattern during southward interplanetary magnetic field using DE 2 data, *J. Geophys. Res.*, *95*(A3), 2333–2343, doi:10.1029/JA095iA03p02333.

Higel, B., and L. Wu (1984), Electron density and plasmapause characteristics at 6.6 RE: A statistical study of the GEOS 2 relaxation sounder data, *J. Geophys. Res.*, *89*(A3), 1583–1601, doi:10.1029/JA089iA03p01583.

Huang, X., B. W. Reinisch, P. Song, J. L. Green, and D. L. Gallagher (2004), Developing an empirical density model of the plasmasphere using IMAGE/RPI observations, *Adv. Space Res.*, *33*, 829–833, doi:10.1016/j.asr.2003.07.007.

Lawrence, D. J., M. F. Thomsen, J. E. Borovsky, and D. J. McComas (1999), Measurements of early and late time plasmasphere refilling as observed from geosynchronous orbit, *J. Geophys. Res.*, *104*(A7), 14,691–14,704, doi:10.1029/1998JA900087.

Lemaire, J. F. (2001), The formation of the light-ion trough and peeling off the plasmasphere, *J. Atmos. Terr. Phys.*, *63*, 1285–1291, doi:10.1016/S1364-6826(00)00232-7.

Lemaire, J. F., and K. I. Gringauz (1998), *The Earth's Plasmasphere*, 372 pp., Cambridge Univ. Press, Cambridge, U. K.

Lemaire, J. F., and R. W. Schunk (1992), Plasmaspheric wind, *J. Atmos. Terr. Phys.*, *54*, 467–477, doi:10.1016/0021-9169(92)90026-H.

McIlwain, C. E. (1986), A *Kp* dependent equatorial electric field model, *Adv. Space Res.*, *6*(3), 187–197, doi:10.1016/0273-1177(86)90331-5.

Mosier, S. R., M. L. Kaiser, and L. W. Brown (1973), Observations of noise bands associated with the upper hybrid resonance by the Imp 6 radio astronomy experiment, *J. Geophys. Res.*, *78*(10), 1673–1679, doi:10.1029/JA078i010p01673.

Nagai, T., J. L. Horwitz, R. R. Anderson, and C. R. Chappell (1985), Structure of the plasmapause from ISEE 1 low-energy ion and plasma wave observations, *J. Geophys. Res.*, *90*(A7), 6622–6626, doi:10.1029/JA090iA07p06622.

Nishida, A. (1966), Formation of plasmapause, or magnetospheric plasma knee, by the combined action of magnetospheric convection and plasma escape from the tail, *J. Geophys. Res.*, *71*(23), 5669–5679.

Park, C. G. (1970), Whistler observations of the interchange of ionization between the ionosphere and the protonosphere, *J. Geophys. Res.*, *75*(22), 4249–4260, doi:10.1029/JA075i022p04249.

Pierrard, V., and K. Stegen (2008), A three-dimensional dynamic kinetic model of the plasmasphere, *J. Geophys. Res.*, *113*, A10209, doi:10.1029/2008JA013060.

Reinisch, B. W., et al. (2000), The Radio Plasma Imager investigation on the IMAGE spacecraft, *Space Sci. Rev.*, *91*, 319–359, doi:10.1023/A:1005252602159.

Reinisch, B. W., X. Huang, P. Song, G. S. Sales, S. F. Fung, J. L. Green, D. L. Gallagher, and V. M. Vasyliunas (2001), Plasma density distribution along the magnetospheric field: RPI observations from IMAGE, *Geophys. Res. Lett.*, *28*, 4521–4524, doi:10.1029/2001GL013684.

Reinisch, B. W., X. Huang, P. Song, J. L. Green, S. F. Fung, V. M. Vasyliunas, D. L. Gallagher, and B. R. Sandel (2004), Plasmaspheric mass loss and refilling as a result of a magnetic storm, *J. Geophys. Res.*, *109*, A01202, doi:10.1029/2003JA009948.

Sandel, B. R., et al. (2000), The Extreme Ultraviolet (EUV) imager investigation for the IMAGE mission, *Space Sci. Rev.*, *91*, 197–242, doi:10.1023/A:1005263510820.

Shaw, R. R., and D. A. Gurnett (1980), A test of two theories for the low-frequency cutoffs of nonthermal continuum radiation, *J. Geophys. Res.*, *85*(A9), 4571–4576, doi:10.1029/JA085iA09p04571.

Singh, N., and J. L. Horwitz (1992), Plasmasphere refilling: Recent observations and modeling, *J. Geophys. Res.*, *97*(A2), 1049–1079, doi:10.1029/91JA02602.

Singh, N., R. W. Schunk, and H. Thiemann (1986), Temporal features of the refilling of a plasmaspheric flux tube, *J. Geophys. Res.*, *91*(A12), 13,433–13,454, doi:10.1029/JA091iA12p13433.

Song, P., B. W. Reinisch, and X. Huang (2004), Magnetospheric active wave measurements, *COSPAR Colloq. Ser.*, *16*, 235–246, doi:10.1016/S0964-2749(05)80036-8.

Su, Y.-J., M. F. Thomsen, J. E. Borovsky, and D. J. Lawrence (2001), A comprehensive survey of plasmasphere refilling at geosynchronous orbit, *J. Geophys. Res.*, *106*(A11), 25,615–25,629, doi:10.1029/2000JA000441.

Thomsen, M. F., J. E. Borovsky, D. J. McComas, and M. R. Collier (1998), Variability of the ring current source population, *Geophys. Res. Lett.*, *25*(18), 3481–3484, doi:10.1029/98GL02633.

Tsyganenko, N. A. (1995), Modeling the Earth's magnetospheric magnetic field confined within a realistic magnetopause, *J. Geophys. Res.*, *100*(A4), 5599–5612, doi:10.1029/94JA03193.

Tu, J., P. Song, B. W. Reinisch, J. L. Green, and X. Huang (2006), Empirical specification of field-aligned plasma density profiles for plasmasphere refilling, *J. Geophys. Res.*, *111*, A06216, doi:10.1029/2005JA011582.

Tu, J., P. Song, B. W. Reinisch, and J. L. Green (2007), Smooth electron density transition from plasmasphere to the subauroral region, *J. Geophys. Res.*, *112*, A05227, doi:10.1029/2007JA012298.

Wilson, G. R., J. L. Horwitz, and J. Lin (1992), A semikinetic model for early stage plasmasphere refilling: 1. Effects of Coulomb collisions, *J. Geophys. Res.*, *97*(A2), 1109–1119, doi:10.1029/91JA01459.

J. B. Cao and H. S. Fu, State Key Laboratory for Space Weather, Center for Space Science and Applied Research, Beijing 100190, China. (huishanf@gmail.com)

B. W. Reinisch, P. Song, J. Tu, and B. Yang, Center for Atmospheric Research, University of Massachusetts Lowell, Lowell, MA 01854, USA.